# *Moquiniastrum polymorphum* subsp. *polymorphum* extract inhibits the proliferation of an activated hepatic stellate cell line (GRX) by regulating the p27 pathway to generate cell cycle arrest

Matheus Scherer Bastos [a,b,*], Rafaela Mallmann Saalfeld [a], Bruna Pasqualotto Costa [a], Maria Claudia Garcia [a], Krist Helen Antunes [c], Kétlin Fernanda Rodrigues [a], Denizar Melo [a], Eliane Romanato Santarém [b], Jarbas Rodrigues de Oliveira [a]

[a] *PUCRS, Laboratório de Biofísica Celular e Inflamação, Porto Alegre, Brazil*
[b] *PUCRS, Laboratório de Biotecnologia Vegetal, Porto Alegre, Brazil*
[c] *PUCRS, Laboratório de Imunologia Clínica e Experimental, Porto Alegre, Brazil*

## ARTICLE INFO

## ABSTRACT

*Ethnopharmacological relevance:* The chosen plant and its extracts have been an alternative in the treatment of several inflammatory and oxidant diseases, and is therefore a viable option for the treatment of hepatic fibrosis.

*Aim of the study:* This study aimed to use *Moquiniastrum polymorphum* subsp. *polymorphum*, mainly the ethanolic extract and fractions, in the treatment of hepatic fibrosis.

*Materials and methods:* Extracts were prepared from dried leaves in 100% ethanol (ET) and fractionated with an increased polarity solvent (dichloromethane to methanol). The quantification of compounds in the extracts was characterized by GCMS. The decrease in cell proliferation and the cytotoxicity of the extracts were evaluated together with the mechanisms of apoptosis and autophagy. The expression of genes associated with decreased fibrosis and cell cycle control was assessed and the production of lipid droplets was quantified by Oil Red O staining.

*Results:* The experiments showed that treatment with ET and fraction 1 (F1) inhibited the expression of CDKIs (CCDN1, CDK2, CDK4 and CDK6) through an increase in p27, related to an increase in autophagic vesicles. The extract and F1 were able to decrease proliferation and revert the activated state of GRX cells to their quiescent state.

*Conclusion:* Our results suggest that extracts obtained from *Moquiniastrum polymorphum* subsp. *polymorphum* have a potential therapeutic effect against liver fibrosis.

## 1. Introduction

The species *Moquiniastrum polymorphum* subsp. *polymorphum* (MP), also known by the synonym *Gochnatia polymorpha* (Less) (GP), corresponds to the latest revision of the MPNS (Medicinal Plant Names Services) and is found in several Latin American countries, although it is mainly found in Brazil. Its flowers, leaves and bark have excellent potential as a source of natural antioxidants and thus have been used in medicine for the treatment of inflammatory diseases of the respiratory tract, muscular diseases such as rheumatism, chronic diseases and cancer (de Moraes Gonçalves et al., 2019; Guarneire et al., 2021; Piornedodos et al., 2011; Teixeira et al., 2016; Youssef et al., 2013). MP has been shown to be a safe anti-inflammatory agent for use during pregnancy, as non-steroidal anti-inflammatory drugs may be abortifacient during their use in pregnancy (David et al., 2014). MP also showed antitumor activity in breast cancer models by treating Walker-256 carcinosarcoma as well as on the MCF7 cell line (human breast cancer cell line) (de Oliveira Mauro et al., 2017; Martins et al., 2015) and also against colorectal carcinogenesis (Limeiras et al., 2017). In this context,

| Abbreviations | |
|---|---|
| AVOs | Acid vesicular organelles |
| B2M | $\beta_2$ microglobulin |
| CIS | Cisplatin |
| ET | Ethanol extract |
| F1 | Fraction 1 |
| F2 | Fraction 2 |
| F3 | Fraction 3 |
| HF | Hepatic fibrosis |
| GP | *Gochnatia polymorpha* |
| GRX | Hepatic stellate cell line |
| HD | Hydroxybenzoic acid |
| HPLC | High performance liquid chromatography |
| HSCs | Hepatic stellate cells |
| LDH | Lactate dehydrogenase |
| MEC | Extracellular matrix |
| MP | *Moquiniastrum polymorphum* subsp. *polymorphum* |
| NAC | N-acetyl cysteine |
| PPARγ | Peroxisome proliferation activated receptor gamma |
| ORO | Oil Red O |
| TGF-β | Transforming growth factor beta |

the unexplored potential of PM as a drug source is enormous, as it has an antimutagenic potential (Oliveira et al., 2016) as well as excellent potential for the treatment of chronic and inflammatory diseases (de Moraes Gonçalves et al., 2019; Piornedodos et al., 2011).

Hepatic fibrosis (HF) is a well-known disease related to chronic liver damage normally caused by inflammatory components. HF can be caused by several factors, such as hepatitis B and C, excessive alcohol use, toxins, metal accumulation and hereditary diseases (Roehlen et al., 2020), resulting in the activation of fibrotic processes in cells known as hepatic stellate cells (HSCs), which have been identified as HF triggers. This activation can alter the phenotypic characteristics of HSCs, resulting in a loss of lipocytic character, which ends up promoting the accumulation of extracellular matrix (ECM) and leads to the destruction of the architecture of the hepatic tissue and, in more severe cases, the development of cirrhosis followed by of liver failure (Friedman, 2008; Wynn and Ramalingam, 2012). HSCs are considered the main cellular structure in the HF process and are usually found in a quiescent state (Wynn and Ramalingam, 2012). Under normal conditions, this quiescent phenotype is maintained by transcription factors, such as peroxisome proliferation activated receptor gamma (PPARγ), which is considered one of the key factors responsible for adipogenic regulation in HSCs (Guimarães et al., 2007; Tsukamoto et al., 2006), de Mesquita et al. (2013); Park et al. (2019). Therefore, the inhibition of HSCs activation appears to be an effective strategy for the therapy of liver fibrosis.

Currently, there are no treatments capable of inactivating stellate cells nor decreasing their proliferation or reversing them to their quiescent state (non-activated state) (Schuppan et al., 2018). The available drugs used for HF treatment are related to antioxidant effects, such as N-acetyl cysteine (NAC), which is widely used for liver regeneration in patients intoxicated with paracetamol. In addition, inhibitors of transforming growth factor-beta (TGF-β), an interleukin that promotes collagen production, are also used to suppress fibrinogenesis, as this growth factor has been shown to activate HSCs, favoring the chronic hepatic inflammatory process, as well as HSC proliferation (Dooley and ten Dijke, 2012; Kolios, 2006; Pereira-Filho et al., 2008).

Therefore, the present study aimed to evaluate the antifibrotic effects and the mechanisms involved in the treatment with MP extracts in HSCs using GRX cells.

## 2. Material and methods

### 2.1. Chemical and reagents

Absolute ethyl alcohol 99.5% (code: A1084/A2228), methanol (code: A1085/A2227) and dichloromethane (code: D1003), which were used to prepare the extract and fractions, were purchased from SYNTH (São Paulo, Brazil). DMEM (Dulbecco's Modified Eagle's Medium; code: 31600-034), fetal bovine serum (FBS; code: 126557-029), penicillin-streptomycin (10,000 U/mL; code: 15140-122), 0.5% trypsin/EDTA (code: 25200-072) solution and trypan blue (code: 68803-612-10) were obtained from Gibco Laboratories (Carlsbad, USA). Acridine orange (C17H19N3; code: 235474) were purchased from Sigma-Aldrich (St. Louis, USA). The lactate dehydrogenase (LDH; code: BT1100400) kit was purchased from Labtest (Minas Gerais, Brazil). Annexin V-FITC and propidium iodide (code: 100034) were provided by Quatro G (Porto Alegre, Brazil). Trizol™ was purchased from Invitrogen (Massachusetts, USA; code: 15596026) and the GoScript kit (code: A5001) used to produce cDNA was purchased from Promega (São Paulo, Brazil). Oil Red O dye used to stain lipid droplets was purchased from Sigma-Aldrich (St. Louis, USA; code: O0625).

### 2.2. Preparation of plant extracts and fractionation

The specimen of M. polymorphum was identified, authenticated by a botanist and deposited in the Herbarium of the Museum of Science and Technology of the Pontifical Catholic University of Rio Grande do Sul – PUCRS (Herbarium MPUC; MPUC 22565). MP was collected in Mariana Pimentel, Rio Grande do Sul, Brazil (30° 21 ′09 ″S; 51° 34 ′59″ W; 119 m). Its leaves were dried at 40 °C and used to prepare the ethanol extract (ET). Dry ground leaves (4 g) were macerated with 100 mL of ethanol/water (80:20; v/v) and kept at room temperature for 7 days. ET was fractionated on a silica chromatography column (stationary phase); the mobile phases consisted of dichloromethane/methanol (90:10; v/v), methanol (100%) and methanol/water (80:20; v/v) solutions, resulting in fractions F1, F2 and F3, respectively. The ethanol extract (ET) and the fractions (F1, F2 and F3) were dried under reduced pressure and then dissolved in DMEM at a concentration of 100 mg/mL.

### 2.3. Cell line and culture conditions

An activated hepatic stellate cell line (GRX; Rio de Janeiro Cell Bank; Brazil) was used for these experiments. Cells were grown in DMEM supplemented with 5% FBS, 0.1% (v/v) fungizone® and 0.5 U/mL penicillin/streptomycin, at 37 °C, 95% relative humidity and 5% $CO_2$ atmosphere. At the time of experimentation, cells were obtained from subconfluent cultures with 0.5% trypsin in 5 mM EDTA, counted on a Neubauer chamber and plated at the appropriate density for each experiment.

### 2.4. Cell viability

Cell viability was determined by the trypan blue exclusion assay (Strober, 2001). In this protocol, a viable cell will present a clear cytoplasm, while a non-viable cell will be identified by a blue cytoplasm. GRX cells were seeded in a 24-well plate at $5 \times 10^3$ per well for 24 h, then treated with different concentrations of ET and its fractions (60–10,000 µg/mL). After 72 h, cells were harvested, suspended in PBS containing trypan blue (1:1), and the percentage of trypan blue positive cells (TBPC) was determined using a Neubauer chamber. The negative control consisted of cells treated with medium, while NAC (400 µg) was used as a positive treatment control. Results are expressed as the percentage of live cells relative to the control group. The percentage of living cells was calculated using the following equation (Eq. (1)):

$$\% \ of \ living \ cells = \left( \frac{\text{TBPC}_{Treated \ cells}}{Mean \ \text{TBPC}_{Untreated \ cells}} \right) \times 100 \qquad \text{Eq. (1)}$$

## 2.5. Cytotoxicity assay

The evaluation of cytotoxicity was performed by assessing the enzyme lactate dehydrogenase (LDH). The LDH assay was performed to assess the cell membrane integrity GRX cells, as LDH release is evidence of membrane disruption (Kumar et al., 2018). GRX cells were seeded at $5 \times 10^3$ per well in 24-well plates and incubated with ET (60 μg/mL) and F1 (60 μg/mL) for 72 h. Enzyme activity was measured in the supernatant and cell lysate by colorimetry using an LDH kit. Tween (5%) was used to control cell lysis. LDH release was measured at 490 nm on a microplate reader (EZ Read 400, Biochrom).

## 2.6. Cell death assay

The identification of necrotic cells, apoptotic cells and early apoptotic cells was performed by flow cytometry (FACS Canto II Flow Cytometer; Becton Dickinson, USA). GRX cells were seeded in a 24-well plate at a density of $5 \times 10^3$ cells per well, treated with ET (60 μg/mL) and F1 (60 μg/mL). After 72 h, the cells were harvested, washed with ice-cold PBS, resuspended in binding buffer (200 μL; 10 mM HEPES)/NaOH, pH 7.4, 140 mM NaCl, 2.5 mM CaCl$_2$), as well as 4 μL of annexin V-FITC and 4 μL of propidium iodide (PI), then incubated at room temperature in the dark for 15 min. Untreated cells were used as a negative control and cells treated with 20 μM cisplatin (CIS) served as a positive control. Data were analyzed using FlowJo 7.6.5 software (Tree Star Inc., Ashland, OR).

## 2.7. Measurement of profibrotic, apoptotic, senescence and cell cycle arrest genes

The expression of genes related to fibrosis (TGF-β, Col-1 and α-SMA), lipid synthesis (PPARγ), apoptosis (pro-apoptotic BAX and antiapoptotic Bcl-2), CDKIs (p53, p21, p27 and p16) and cell cycle arrest (CCND1 and CDK2, CDK4 and CDK6) was assessed. GRX cells were seeded at $10 \times 10^4$ cells per well in 6-well plates and cultured for 24 h. Then, the cells were treated with ET (60 μg/mL) and F1 (60 μg/mL) for 72 h. Total RNA from controls and treated GRX cells was extracted using Trizol and cDNA was synthesized using the GoScript reverse transcription kit following the manufacturer's instructions. cDNA quantification was performed using NanoDrop 2000 (Thermo Fisher Scientific). A total of 64 ng of cDNA from each sample was used for the analysis of relative gene expression in quantitative real-time PCR (qPCR, Step One Plus, Applied Biosystems) using the green fluorescence marker SYBR Green. The relative expression of mRNA was calculated by the delta-delta Ct (ΔΔCt) method. B2M (β$_2$ microglobulin mouse gene) was used as an internal control to normalize RNA variation. The primers used to assess the expression of genes related to senescence and cell cycle arrest are shown in Table 1. The samples were analyzed in duplicate.

## 2.8. Evaluation of acidic vesicular organelles (AVOs)

The quantification of AVOs was performed to study autophagy. GRX cells were seeded at a density of $5 \times 10^3$ cells per well in a 24-well plate, treated with ET (60 μg/mL) and F1 (60 μg/mL) for 72 h. For a positive control for autophagy, cells were treated with rapamycin (RAPA; 10 nM). Untreated GRX cells represent the control group. After 72 h, cells were incubated in a culture medium supplemented with acridine orange (1 μg/mL) for 15 min in the dark at room temperature. Analysis was performed by flow cytometry (FACS Canto II, Becton Dickinson, USA). Data were analyzed using FlowJo v. 7.2.5 (Tree Star Inc., Ashland, OR).

**Table 1**
Sequence of primers used for qPCR.

| Gene | Primer sequences (5′-3′) | Reference |
|------|--------------------------|-----------|
| B2M | F: ACAGTTCCACCCGCCTCACATT | Stepanenko et al. (2022) |
| | R: TAGAAAGACCAGTCCTTGCTGAAG | |
| p53 | F: TGCTCACCCTGGCTAAAGTT | Bassiony et al. (2014) |
| | R: AATGTCTCCTGGCTCAGAGG | |
| p16 | F: TTGGCCCAAGAGCGGGGACA | Bassiony et al. (2014) |
| | R: GCGGGCTGAGGCCGGATTTA | |
| p21 | F: CTGTCTTGCACTCTGGTGTCTGA- | Teratake et al. (2016) |
| | R: CCAATCTGCGCTTGGAGTGA | |
| p27 | F: CAAAACCGAACAAAAGCGAAACGCCA | Teratake et al. (2016) |
| | R: GATACTCTCCCCTTCCTTTGCCTTGTC | |
| CCDN1 | F: GCGTACCCTGACACCAATCTC | Teratake et al. (2016) |
| | R: ACTTGAAGTAAGATACGGAGGGC | |
| CDK2 | F: ACCTCCCGCAGTGTTCCTATT | Teratake et al. (2016) |
| | R: CACAGACCTCTAGCATCCAGG | |
| CDK4 | F: ACTGGCGCATCAGATCCTTA | Teratake et al. (2016) |
| | R: GGAGGCCTTTGAACATCCCA | |
| CDK6 | F: GCTGACCAGCAGTACGAATG | Teratake et al. (2016) |
| | R: GCACACATCAAACAACCTGACC | |
| BCL-2 | F: GTGGATGACTGAGTACCT | Ghatei et al. (2017) |
| | R: CCAGGAGAAATCAAACAGAG | |
| BAX | F: CTACAGGGTTTCATCCAG | Ghatei et al. (2017) |
| | R: CCAGTTCATCTCCAATTCG | |
| TGF-β | F: GGGAAATTGAGGGCTTTCGC | de Souza Basso et al. (2021) |
| | R: TGAACCCGTTGTCCACT | |
| Col-1 | F: AGTGGTTTGGATGGTGCCAA | de Souza Basso et al. (2021) |
| | R: GCACCATCATTTCCACGAGC | |
| α-SMA | F: TAGCACCCAGCACCATGAAG | de Souza Basso et al. (2021) |
| | R: CTGCTGGAAGGTGGACAGAG | |
| PPARγ | F: CTACAGGGTTTCATCCAG | de Souza Basso et al. (2021) |
| | R: CCAGTTCATCTCCAATTCG | |

## 2.9. Oil Red O assay

Phenotypic reversion in hepatic stellate cells was observed using the Oil Red O assay. Cells were plated in a 24-well tissue culture plates ($3 \times 10^3$ cells/well); after 72 h, cells were fixed with 10% formaldehyde for 1 h then stained with Oil Red O (ORO) (Sigma Chemical), after 30 min Intracellular lipid accumulation were observed using an inverted light microscope at a magnification of 400x. For the estimation of lipid accumulation, the ORO within the lipid droplets was extracted using isopropanol; the absorbance was read at a wavelength of 492 nm using an ELISA plate reader. Specific lipid content was calculated as the ratio of absorbance value obtained for ORO and the number of cells.

## 2.10. Analysis of protein expression (western blot)

From the cell culture samples, the proteins were extracted with the lysis buffer (CHAPS) and separated in polyacrylamide gel in vertical electrophoresis. After performing the electrophoresis, the proteins were transferred to a nitrocellulose membrane and incubated with different antibodies. The primary antibodies were anti-GPDH, anti-BAX, anti-mTOR and anti-α-SMA. Subsequently, the samples were incubated with secondary antibodies Anti - IgG conjugated with peroxidase, which react with a chemiluminescent substrate. The development of the bands was evaluated using the ImageJ software.

## 2.11. Identification of components in the crude extract and fractions

The profile of ET and F1 compounds was analyzed by Gas Chromatography coupled to mass spectrometry (GCMS). The dry extracts were solubilized in 2 mL of ethanol, extracted with ultrasound and filtered through a 0.22 μm cellulose acetate filter. The compounds are presented in relation to the retention times (peaks), area values and the name of the compound. The mass spectral library (National Institute of Standards and Technology - NIST) was used to identify the compounds of ET and F1. The relative percentage of each compound in relation to all compounds identified in the analyzed sample is also presented.

## 2.12. Statistical analysis

Results are expressed as mean ± standard error. Data were analyzed by one-way analysis of variance (ANOVA) and means were separated by the Tukey posthoc test ($p < 0.05$). Statistical analyses were performed using GraphPad Prism 8.0 Software.

## 3. Results

### 3.1. Effect of the ethanol extract and its fractions on GRX cell proliferation

The antiproliferative effect of the ethanol extract and fractions was evaluated in GRX cells treated with increasing concentrations of ET, F1, F2 and F3 (60, 125, 250, 500, 1000, 2500, 5000 and 10000 μg/mL). It was possible to see that treatment with ET and the fractions resulted in a significant decrease in cell number (Fig. 1A–D). On the one hand, ET showed promising antiproliferative activity, as its lowest concentration, 60 μg/mL, managed to reduce 50% of GRX cells, while F1 showed antiproliferative activity equivalent to ET at the same concentration. Consequently, the latter was considered the best fraction, since F2 reduced the GRX population by 40% and F3 was able to decrease this by 11%. Therefore, ET and F1 were further used at a concentration of 60 μg/mL, which was the lowest significant concentration for the same extracts, in the following experiments.

### 3.2. Effect of ethanol extract and F1 fraction on the integrity of GRX cells

Cell membrane integrity was evaluated to rule out the possibility that the antiproliferative effect was not associated with membrane damage related to cell death caused by necrosis (Fig. 2). Thus, the lowest concentration with antifibrotic activity common to all extracts/fractions was selected. ET (60 μg/mL) and F1 (60 μg/mL) treated GRX cells did not result in significant LDH release, indicating that no membrane damage was occurring in these cells in response to treatment. Therefore, concentrations of 60 μg/mL for ET and F1 were chosen for the following
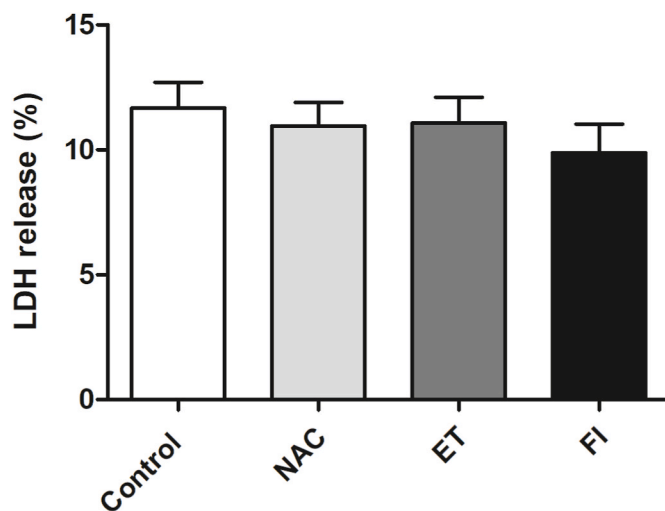


**Fig. 2.** The effect of membrane integrity ET (60 μg/mL), F1 (60 μg/mL) and NAC (400 μg/mL) was evaluated by measuring the levels of LDH released. Data represent mean ± SD (n = 4). Results are expressed as percentage of cells.

experiments.

### 3.3. ET and F1 do not induce apoptosis

To determine a possible mechanism for the reduction of cell proliferation, the process of cell death by apoptosis was evaluated. A significant decrease was observed between the treatments and the control (only cells) and positive controls (cells + cisplatin 20 μM) (Fig. 3 A–D).

### 3.4. ET and F1 induce anti-apoptotic genes and proteins

To confirm the previous results on the decrease in apoptosis of GRX cells with ET and F1 treatments, the BAX (pro-apoptotic) and BCL-2
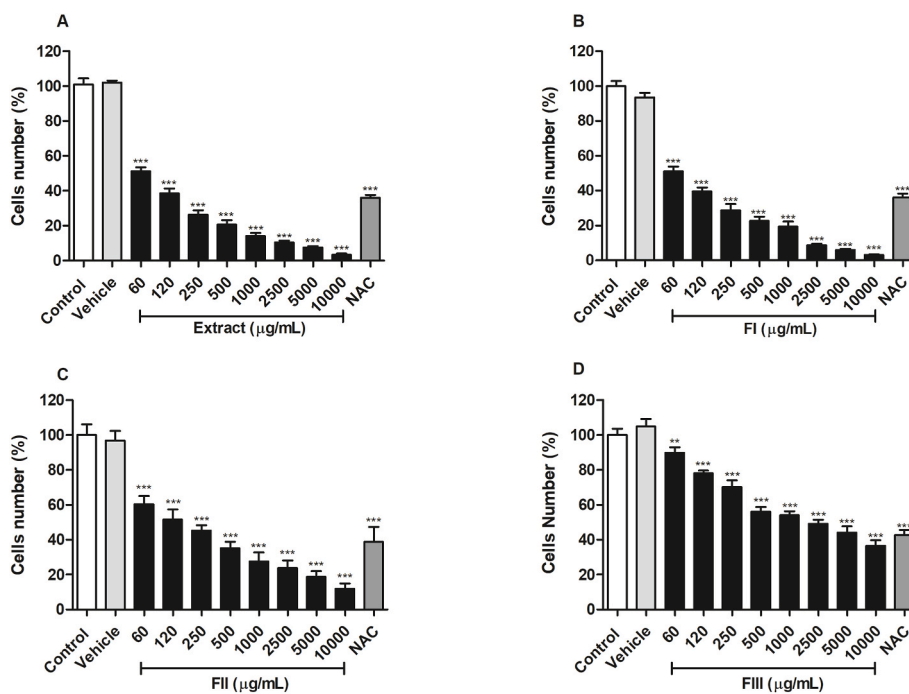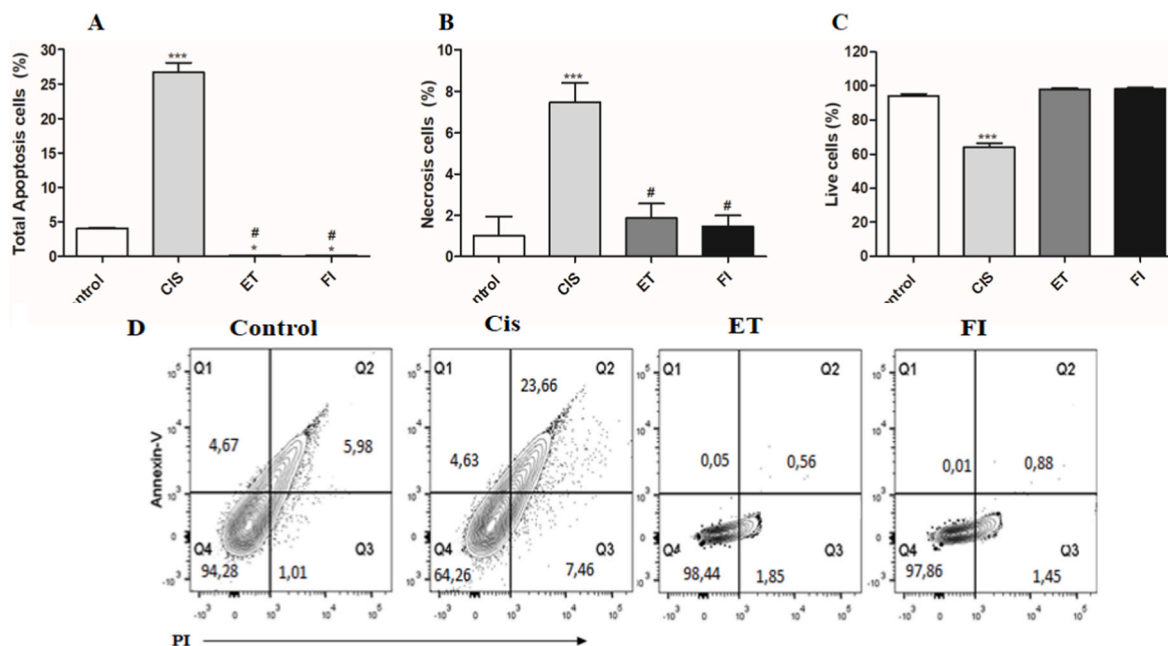


**Fig. 1.** Effect of ET and its fractions on cell proliferation after 72 h. (A) Ethanol extract, (B) F1, (C) F2 and (D) F3 at concentrations of 60, 125, 250, 500, 1000, 2500, 5000 and 10000 μg/mL. NAC was used as a positive control (400 μg/mL) to decrease proliferation. Cell proliferation was assessed by the trypan blue exclusion method. **P < 0.01 and ***P < 0.001 compared to control.

**Fig. 3.** Effect of ET and F1 on apoptosis. Cells were exposed to ET (60 μg/mL) and F1 (60 μg/mL) and analyzed for the occurrence of (A) total apoptosis, (B) necrosis and (C) normal cells. Cisplatin (20 μM) was used as a positive control. (D) Representative flow cytometry plots of PI (x-axis)/Annexin V (y-axis). Results are expressed as the percentage of apoptotic cells. Data represent mean ± SD (n = 4). *P < 0.05 and ***P < 0,001 compared to control. #P < 0.05 compared to CIS 20 μM as the positive control.

(anti-apoptotic) genes were evaluated (Fig. 4A). We observed that there was an increase in the expression of the BCL-2 gene in relation to the control group and a reduction in the BAX gene in relation to the CIS group, confirming that the treatments did not induce apoptosis. We also evaluated BAX expression using Western blot. The results confirmed that the treatments did not induce apoptosis (Fig. 4B–C).

### 3.5. Treatments induce cell cycle arrest by downregulating cyclin-dependent kinases

Since the extract and its fractions did not provoke apoptosis, we decided to evaluate cell cycle alterations. Cyclins and cyclin-dependent kinases (CDKs) are the main factors required for cell cycle progression (CCP) and the proteins p16, p53, p21 and p27 (CDK inhibitors) provoke cell cycle arrest (CCA). Therefore, the expression of CCND1 (cyclin D1) as well as CDK2, CDK4 and CDK6 (cyclin-dependent kinases) was evaluated. ET and FI treatments decreased the expression of CCND1 (Fig. 5A) as well as CDK2, CDK4 and CDK6 (Fig. 5B–D), demonstrating

that these treatments could induce cell cycle arrest by downregulating CDKs.

### 3.6. ET and F1 do not alter the expression of the p53, p21 and p16 genes, but increase the expression of the p27 gene

After to see those treatments with ET and F1 were able to decrease cyclin levels and CDK's, we investigate their regulation by CDK inhibitors (CDKIs). There are two known families of CDKIs, i.e. the INK4 inhibitors (p16/INK4A, p15/INK4B, p18/INK4C and p19/INK4D) and the CIP/KIP inhibitors (p21/CIP1, p27/KIP1 and P57/KIP2). The gene expression p16, p53, p21 and p27 was investigated. It was found that p53, p21 and p16 gene expression did not increase in response to treatment with ET and F1 (Fig. 6A–C). However, treatment with ET and F1 was able to increase p27 expression (Fig. 6D).
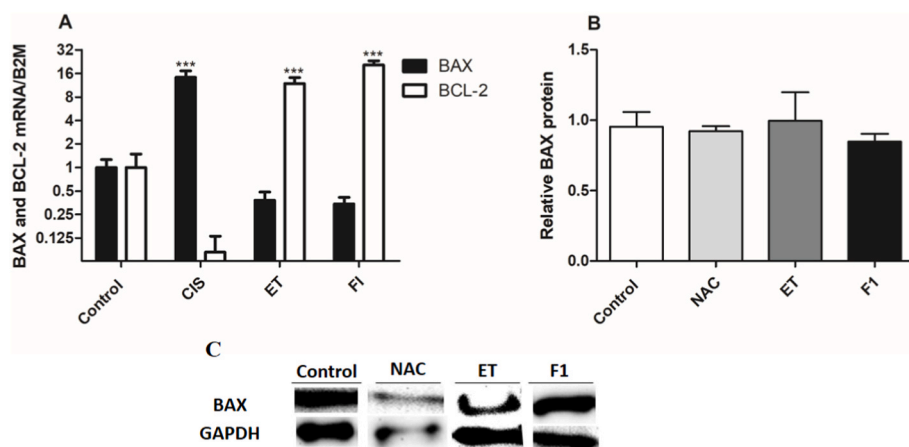


**Fig. 4.** Effect of ET (60 μg/mL) and F1 (60 μg/mL) on BAX (pro-apoptotic) and BCL-2 (anti-apoptotic) gene expression (A) and BAX protein expression (B–C) in GRX cells after 72 h of treatment. Cisplatin (20 μM) was used as a positive control. B2M was used as an internal control for gene expression and GAPDH was used as an internal control for protein expression by W. Blot. Results are expressed as target gene/B2M, and data represent mean ± SD (n = 4). ***p < 0.001 in relation to the control. #P < 0.05 compared to 20 μM CIS as a positive control.
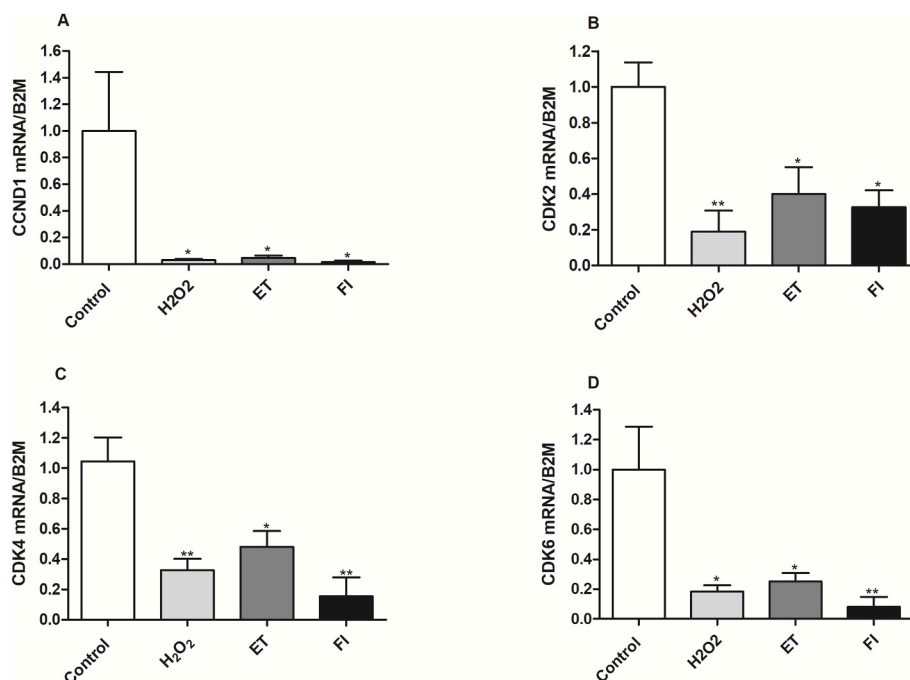
**Fig. 5.** Effect of ET (60 μg/mL) and F1 (60 μg/mL) on the expression of genes encoding cell cycle progression in GRX cells after 72 h of treatment. Relative expression of (A) CCND1, (B) CDK2, (C) CDK4 and (D) CDK6 mRNA in the treatment groups. $H_2O_2$ (150 μM) was used as a positive control. B2M was used as an internal control. Results are expressed as target gene/B2M and data represent mean ± SD (n = 4). *p < 0.05 and**p < 0.01 in relation to control.
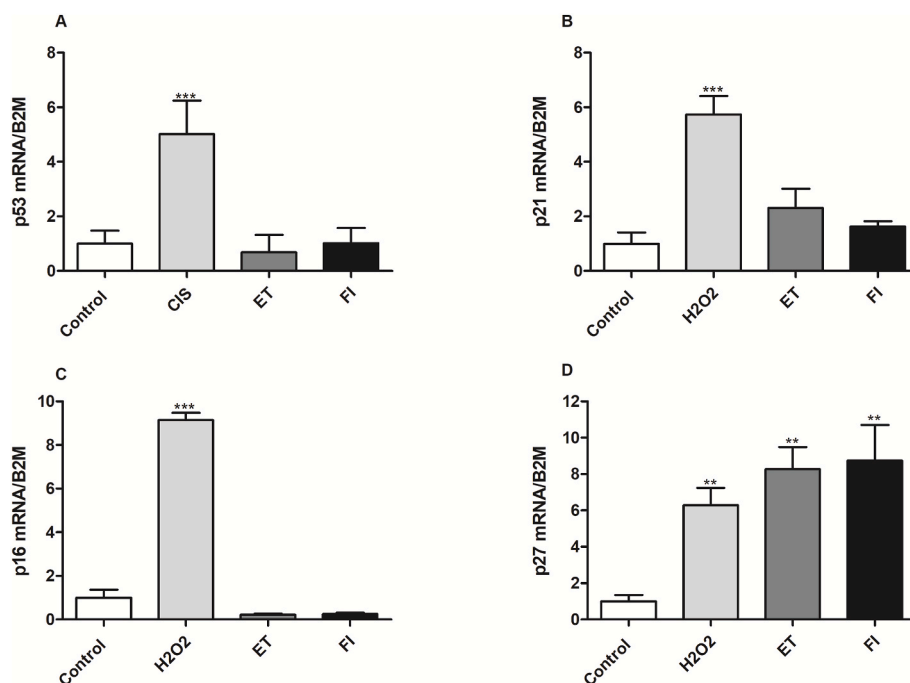


**Fig. 6.** Effect of ET (60 μg/mL) and F1 (60 μg/mL) on the expression of genes encoding cell growth regulators in GRX cells after 72 h of treatment. Relative expression of mRNA(A) p53, (B) p21, (C) p16 and (D) p27 in treatment groups. CIS (25 μM) and $H_2O_2$ (150 μM) was used as a positive control. B2M was used as an internal control. Results are expressed as target gene/B2M and data represent mean ± SD (n = 4). **p < 0.01 and ***p < 0.001 in relation to control.

### 3.7. mTOR reduction is involved in ET and F1-induced cell cycle arrest

mTOR is a classical pathway involved in numerous cellular functions, including cell proliferation and cell cycle progression by inhibiting cell apoptosis and promoting cell proliferation (Sui et al., 2021; Zhang et al., 2017). Thus, mTOR protein expression was evaluated by western blotting. The result showed that mTOR expression was decreased by treatment with ET and F1 (Fig. 7A–B).

### 3.8. ET and F1 increase acidic vesicular organelles in GRX cells

Autophagy is a process that plays a key role in preserving biological processes and decreasing cell proliferation in defective cells (Calzadilla et al., 2011). Taking into account this information, we evaluated the
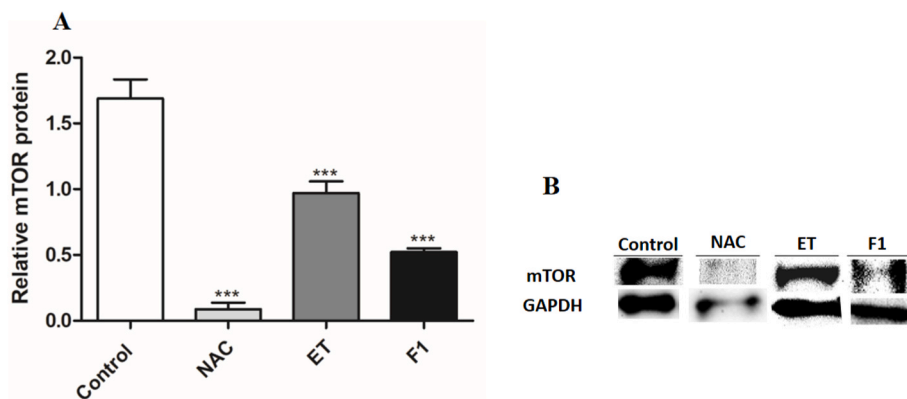
**Fig. 7.** Effect of ET (60 μg/mL) and IF (60 μg/mL) on (A) mTOR protein expression in GRX cells after 72 h of treatment. (B) GAPDH was used as an internal control for protein expression. Results indicate target gene/GAPDH and data represent mean $\pm$ SD (n = 4). ***p < 0.001 compared to the control.

induction of autophagy by ET and F1 through the formation of acidic vesicular organelles (AVOs) (Fig. 8A–B), due to the relationship between cell cycle arrest and autophagy. Treatment with ET and F1 increased the percentage of AVOs in GRX cells (Fig. 8A). Treatment with rapamycin (RAPA; 1 μM) was used as a positive control and promoted a significant increase in AVOs. Thus, AVO formation suggests that the increase in lysosomal content is a cellular response induced by ET and F1 in GRX cells.

### 3.9. ET and F1 can reverse the activated phenotype of GRX myofibroblasts

It is believed that two possible pathways exist to decrease hepatic fibrosis. The first # is to decrease cell proliferation and the second is to reverse cell phenotype. Aimed at investigating the capacity of the ET and F1fraction in the reversal of GRX cell phenotype, i.e. inducing lipid accumulation in the cytoplasm, the cells were observed and quantified by ORO staining. Both treatments induced GRX cells to increase fat

storage capacity in the cytoplasm (Fig. 9C) and quantified absorbance at 492 nm (Fig. 9A). NAC treatment also induced lipid accumulation in the cytoplasm (Fig. 9A–C). Considering that staining with ORO revealed the formation of fat droplets, the expression of PPARγ, which is a lipid synthesis-related gene, was determined, thus elucidating the phenotypic reversal mechanism pathway. Compared to the control group, the treated groups showed a significant increase in PPARγ mRNA expression, suggesting that the investigated treatments are involved in lipid droplet accumulation in the GRX cell cytoplasm (Fig. 9B).

### 3.10. ET and F1 reduce extracellular matrix components

After verifying that the treatments were able to induce the production of lipid droplets in GRX cells, the ability of ET and F1 was also found to be able to decrease gene expression in pro-fibrotic genes such as TGF-β (Fig. 10A), Col-1 (Fig. 10B) and α-SMA (Fig. 10C). Furthermore, we show that ET and F1 decreased α-SMA protein expression, corroborating our findings about gene expression (Fig. 10D–E).
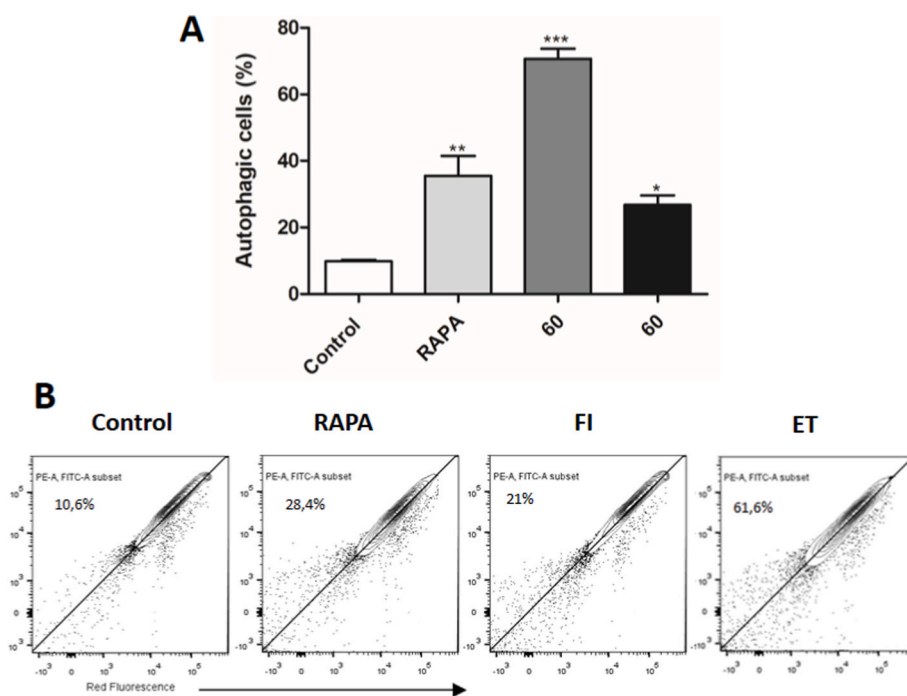


**Fig. 8.** Effect of extract and fractions on cellular autophagy. (A) Cells were exposed to ET (60 μg/mL) and F1 (60 μg/mL) or RAPA (1 μM) as the positive control. (B) Representative flow cytometry plots of FITC (x-axis)/PerCP (y-axis) to assess autophagy. Data represent mean $\pm$ SD (n = 4). *P < 0.05, **P < 0.01 and ***P < 0.001 compared to the control with only medium and cells.
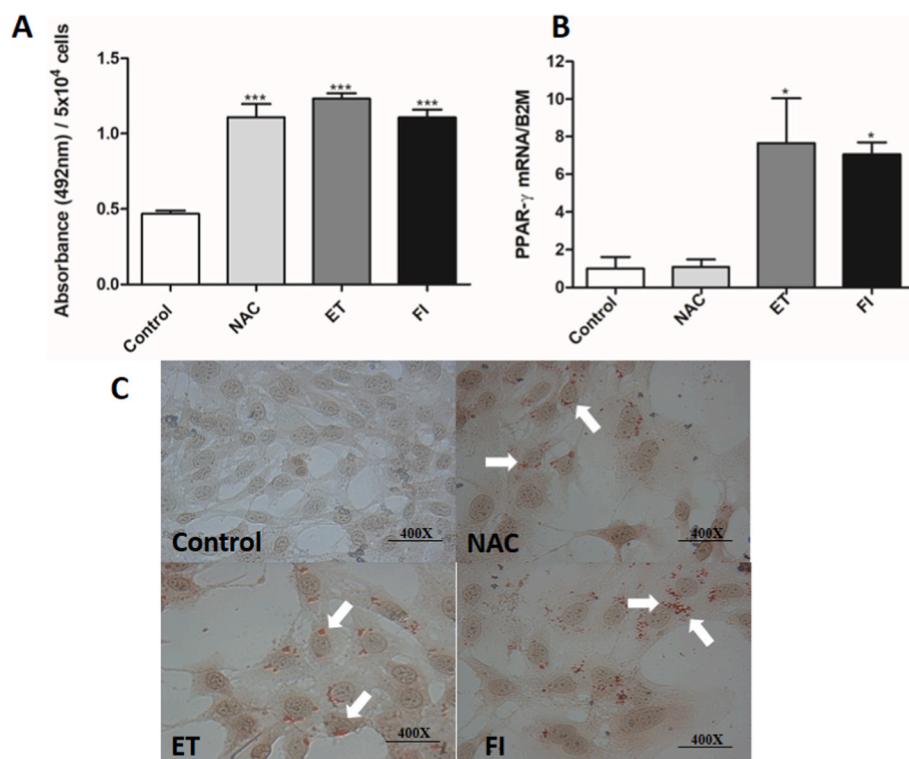
**Fig. 9.** Staining, lipid quantification and mRNA expression of PPARγ after 72 h of treatment. (A) Quantitative results of the treatment with ET (60 μg/mL) and F1 (60 μg/mL) performed by the quantification of the lipid droplets dissolved in isopropyl alcohol (active absorbance value for ORO adjusted for the number of cells $5 \times 10^4$). NAC was used as the positive control (400 μg). (C) Qualitative results obtained by evaluating lipid droplets stained with Oil Red O (400x magnification); lipid droplets are indicated by arrows. (B) Effect of ET and F1 on PPARγ mRNA expression after 72 h of treatment. Results are expressed as target gene/B2M and data represent mean ± SD (n = 4). *p < 0.05 and ***p < 0.001 compared to control. (For interpretation of the references to color in this figure legend, the reader is referred to the Web version of this article.)
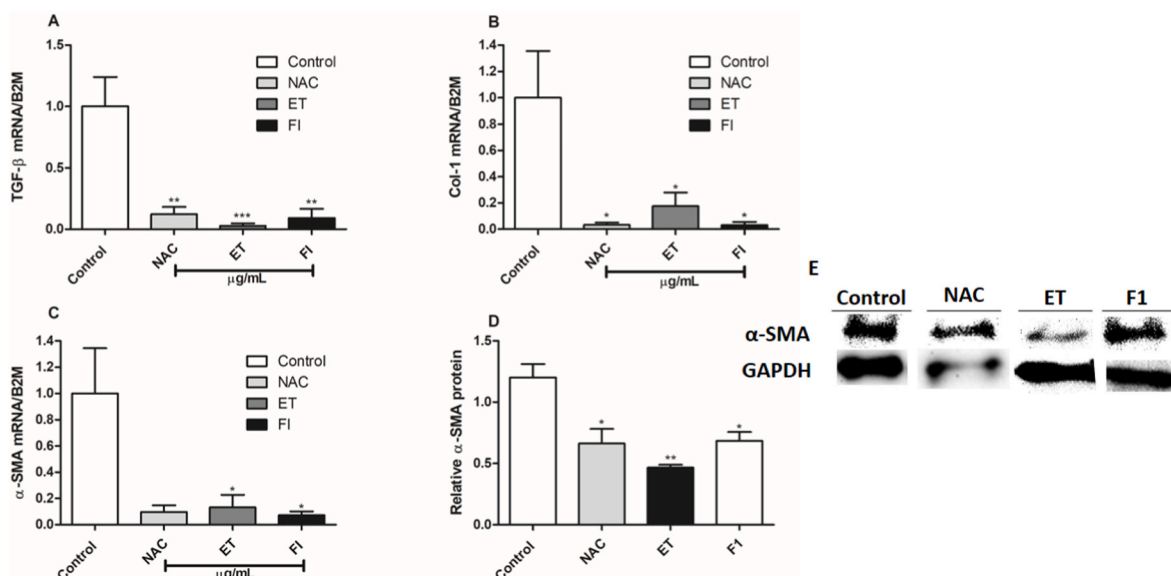


**Fig. 10.** Effect of ET (60 μg/mL) and IF (60 μg/mL) on the expression of pro-fibrotic genes in GRX cells after 72 h of treatment. Relative expression of (A) TGF-β, (B) COL-1, (C) α-SMA mRNA in treatment groups. (D–E) α-SMA protein expression by W. Blot. NAC was used as a positive control (400 μg). B2M was used as an internal control for gene expression and GAPDH was used as an internal control for protein expression. Results indicate target gene/B2M and data represent mean ± SD (n = 4). *p < 0.05, **p < 0.01 and ***p < 0.001 in relation to the control.

### 3.11. Phytochemical analysis of M. polymorphum extract and fractions

The main chemical compounds found in the extract ethanol and fraction 1 are shown in Tables 2 and 3 respectively. The phytochemical analysis of ET from MP showed the presence of 49 phytochemical compounds, being the majority compounds Palmitic acid (10.57%), Ethyl acetoacetate (9.90%) and Valeric acid (7.51%). The phytochemical analysis of F1 found 40 compounds, where the major ones were Coniferyl (12.21%), Palmitic acid (10.31%) and Adipic acid (8.51%). In

Fig. 11A and B we can see the chromatographic profile of ET and F1, respectively.

### 4. Discussion

The Asteraceae family is one of the largest families of flowering plants, having been used in the diet and medicine for centuries for their antioxidant, anti-inflammatory as well as diuretic and healing properties, which are attributed to their range of phytochemical compounds,

**Table 2**
Phytochemical compounds detected in *M. polymorphum* of ET by GCMS.

| Peak# | R.Time (mim) | Compounds (%) | Name | Synonyms | Molecular Formula |
|---|---|---|---|---|---|
| 1 | 4.432 | 2.17 | 2-Propanone, 1,1-dimethoxy- | Dimethoxyphenylacetone/Anisyl propionate | C11H14O3 |
| 2 | 5.215 | 1.17 | Butanoic acid, 3-methyl | Valeric Acid | C5H10O2 |
| 3 | 5.695 | 9.90 | Pentanoic acid, 3-oxo-, methyl ester | Ethyl acetoacetate | C6H10O3 |
| 4 | 5.870 | 7.51 | Butanoic acid, 2-methyl | Valeric acid | C5H10O2 |
| 5 | 5.981 | 5.84 | 1-Methyl-3-pyrrolidinol | N,N-Dietilformamida | C5H11NO |
| 6 | 6.149 | 1.54 | 1-Butanol, 3-methyl-, acetate | Ethyl pentanoate | C7H14O2 |
| 7 | 7.503 | 0.74 | 1,2-Cyclopentanedione | Ethyl propiolate | C5H6O2 |
| 8 | 9.763 | 3.35 | But-3-enyl (E)-2-methylbut-2-enoate | Cyclohexyl acrylate | C9H14O2 |
| 9 | 9.830 | 1.30 | 3-Hexenoic acid, (E)- | Acetonylacetone | C6H10O2 |
| 10 | 10.395 | 0.75 | 1-Acetyl-1,4-dihydropyridine | p-Anisidine | C7H9NO |
| 11 | 11.815 | 0.81 | 2-Pyrrolidinone | Pyrrolidone | C4H7NO |
| 12 | 12.579 | 2.27 | Caprolactam | Aminocaproic Lactam | C6H11NO |
| 13 | 13.195 | 1.18 | 5 4-(4-Methyl-piperazin-1-yl)-1,5,-dihydro-imidazole | Carcinine | C8H14N4O |
| 14 | 13.705 | 0.88 | Succinimide | Methyl cyanoacetate | C4H5NO2 |
| 15 | 14.176 | 0.50 | 4H-Pyran-4-one, 2,3-dihydro-3,5-dihydroxy-6- | 2,3-Dimethylfumaric acid | C6H8O4 |
| 16 | 14.540 | 2.79 | 1-Piperazineethanamine, 4-methyl | Dehydrospermidine | C7H17N3 |
| 17 | 15.048 | 0.90 | Methanol, oxo-, benzoate | Formyl benzoate | C8H6O3 |
| 18 | 15.533 | 5.67 | N-Methylpyrrole-2-carboxylic acid | Ethyl cyanoacrylate | C6H7NO2 |
| 19 | 16.132 | 1.14 | 1,4:3,6-Dianhydro-.alpha.-d-glucopyranose | Dimethyl fumarate | C6H8O4 |
| 20 | 16.450 | 1.19 | Benzofuran, 2,3-dihydro | Flavan | C15H14O |
| 21 | 16.900 | 0.92 | Oxamide, N-(2-morpholinoethyl)- | Oxamide | C8H15N3O3 |
| 22 | 17.122 | 0.71 | Glutamine | L-glutamine | C5H10N2O3 |
| 23 | 17.434 | 3.60 | Benzeneacetic acid | Phenylacetic acid | C8H8O2 |
| 24 | 18.146 | 0.55 | 2-Methyl-4-pyridinamine 1-oxide | 2,4-diaminophenol | C6H8N2O |
| 25 | 19.063 | 1.17 | 1-Amino-4-(2-hydroxyethyl)piperazine | Diethylaminomethylurea | C6H15N3O |
| 26 | 19.095 | 1.26 | 2-Methoxy-4-vinylphenol | Ethyl benzoate | C9H10O2 |
| 27 | 20.110 | 1.92 | Phenol, 2,6-dimethoxy | Eusiderin | C22H26O6 |
| 28 | 22.155 | 1.35 | 5-Hydroxypipecolic acid | N-hydroxypipecolic acid | C8H10O3 |
| 29 | 22.528 | 0.94 | 2-Pyrazolin-5-ol, 5-tridecafluorohexyl-1-(2-hydroxybenzoyl)-3-methyl | – | C17H11F13N2O3 |
| 30 | 25.472 | 0.52 | 3-tert-Butyl-4-hydroxyanisole | BHA | C11H16O2 |
| 31 | 27.408 | 0.81 | Methyl-(2-hydoxy-3-ethoxy-benzyl)ether | 2,4,6-Trimethoxytoluene | C10H14O3 |
| 32 | 27.622 | 0.62 | 2-Butanone, 4-(2,6,6-trimethyl-1-cyclohexen-1-yl)- | Solanone | C13H22O |
| 33 | 29.373 | 3.39 | 3 4-((1E)-3-Hydroxy-1-propenyl)-2-methoxyphenol | Coniferyl | C10H12O3 |
| 34 | 29.686 | 0.55 | Tetradecanoic acid | Myristic acid | C14H28O2 |
| 35 | 30.062 | 1.34 | Widdrol hydroxyether | – | C15H26O2 |
| 36 | 30.246 | 0.53 | (1R,2R,3S,5R)-(−)-2,3-Pinanediol | Citronellic acid | C10H18O2 |
| 37 | 32.014 | 0.43 | 1,2-Benzenedicarboxylic acid, bis(2-methylpropyl) ester | Dibutyl phthalate | C16H22O4 |
| 38 | 32.561 | 0.53 | 3,5-Dimethoxy-4-hydroxyphenethylamine | Tenuazonic acid | C10H15NO3 |
| 39 | 33.744 | 10.57 | n-Hexadecanoic acid | Palmitic acid | C16H32O2 |
| 40 | 35.115 | 0.98 | Undecanoic acid | Methyl decanoate | C11H22O2 |
| 41 | 36.592 | 0.46 | Phytol | (E)-Phytol | C20H40O |
| 42 | 36.937 | 1.41 | 9,12-Octadecadienoic acid (Z,Z)- | Linoleic acid | C18H32O2 |
| 43 | 37.064 | 3.15 | 9,12,15-Octadecatrienoic acid, (Z,Z,Z)- | Alpha-linolenic acid | C36H60O4 |
| 44 | 37.434 | 5.58 | Octadecanoic acid | Stearic acid | C18H36O2 |
| 45 | 38.176 | 1.09 | Andrographolide | Andrographis | C20H30O5 |
| 46 | 38.973 | 1.66 | Benzyl.beta.-d-glucoside | – | C13H18O6 |
| 47 | 43.176 | 0.94 | Hexadecanoic acid, 2-hydroxy-1-(hydroxymethyl)ethyl ester | Glyceryl palmitate | C19H38O4 |
| 48 | 44.357 | 0.99 | Butanoic acid, 2-methyl-, 2-methoxy-4-(2-propenyl)phenyl ester | Parthenolide | C15H2OO3 |
| 49 | 48.721 | 2.52 | Stigmasterol | b-stigmasterol | C29H48O |

including polyphenols, phenolic acids, flavonoids, and acetylenes and triterpenes. In this sense, MP (Asteraceae) has been reported to have anti-inflammatory properties and has been used to treat chronic diseases both in folk medicine and in scientific studies (David et al., 2014; Piornedodos et al., 2011; Teixeira et al., 2016).

Our research evaluated the anti-fibrotic potential of ET and F1 of MP, and we obtained a decrease in the growth of GRX cells. The results showed that the antiproliferative activity of MP in ET and F1 was not associated with membrane damage, indicating that the decrease in fibrotic cells was not due to necrosis. This finding demonstrates the promising anti-fibrotic and non-cytotoxic effect of ET and F1 against activated stellate cell proliferation.

As the treatments with ET and F1 reduced cell proliferation, we aimed to establish the mechanism responsible for this effect, evaluating GRX cell death by apoptosis. Regarding apoptosis, the reduction in the number of cells observed in response to treatment with ET and F1 was not due to this cellular mechanism or to the activation of necrosis-induced programmed cell death. The absence of necrosis by flow

cytometry corroborates the results of the LDH enzyme leakage experiment, demonstrating that the compounds were not cytotoxic at the dose used in this study. To certify that the treatment did not cause apoptosis in GRX cells, we evaluated the gene expression of BAX and BCL-2. In apoptosis, activation of the BAX gene occurs (protein X associated with BCL-2), which incites the opening of mitochondrial ion channels which permeabilizes the outer membrane, leading to the activation of caspases. This mechanism causes inhibition of the anti-apoptotic protein BCL-2, which is extremely important for apoptotic process to continue (Edlich, 2018). Our results showed a decrease in the expression of the BAX gene and protein and an increase in the expression of the BCL-2 gene, corroborating the results obtained by flow cytometry that showed that the treatments did not provoke apoptosis. In addition, treatment with cisplatin (positive control) activated BAX and decreased the expression of the BCL-2 gene; with this treatment, GRX cells underwent cell death by apoptosis.

Since the decrease in proliferation was not due to apoptosis, we investigated whether this decrease was related to cell cycle arrest.

**Table 3**
Phytochemical compounds detected in *M. polymorphum* of F1 by GCMS.

| Peak# | R.Time (mim) | Compounds (%) | Name | Synonyms | Molecular Formula |
|---|---|---|---|---|---|
| 1 | 3.942 | 1.56 | Acetylacetone | Tiglic acid | C5H8O2 |
| 2 | 4.096 | 1.27 | Ethanol, 2-methoxy-, acetate | 3-Hydroxypentanoic acid | C5H10O3 |
| 3 | 4.306 | 1.09 | Butanoic acid, ethyl ester | Hexanoic acid | C6H12O2 |
| 4 | 4.429 | 1.70 | Formamide, N-methoxy- | 4-Phthalimidobutyric acid | C12H11NO4 |
| 5 | 5.275 | 1.57 | 2-Pentanone, 4-hydroxy-4-methyl- | Diacetone alcohol | C6H12O2 |
| 6 | 6.162 | 4.95 | 1-Butanol, 3-methyl-, acetate | Ethyl pentanoate | C7H14O2 |
| 7 | 6.287 | 0.62 | 2-Butanone, 3,4-epoxy-3-ethyl- | Acetonylacetone | C6H10O2 |
| 8 | 9.554 | 1.01 | Pyridine, 2,4,6-trimethyl- | Phenylethylamine | C8H11N |
| 9 | 9.696 | 0.56 | 3-Hexenoic acid, (E)- | Hexane-2,5-dione | C6H10O2 |
| 10 | 9.914 | 0.37 | 1,3-Dioxolane-2-methanol, 2,4-dimethyl- | 2,4-Dimethyl-1,3-dioxolane-2-methanol | C6H12O3 |
| 11 | 10.311 | 0.47 | 2-Cyclohexen-1-one | Cyclohexenone | C6H8O |
| 12 | 11.522 | 0.79 | Pentanoic acid, 4-oxo- | Levulinic acid | C5H8O3 |
| 13 | 13.058 | 3.72 | 2-Oxooctanoic acid | Butyric anhydride | C8H14O3 |
| 14 | 13.196 | 8.52 | alpha.-Hydroxyisobutyric acid, acetate | Adipic acid | C6H10O4 |
| 15 | 14.165 | 1.39 | 4H-Pyran-4-one, 2,3-dihydro-3,5-dihydroxy-6-methyl- | 2,3-Dimethylfumaric acid | C6H8O4 |
| 16 | 15.180 | 2.09 | N-Methylpyrrole-2-carboxylic acid | Ethyl 2-cyanoacrylate | C6H7NO2 |
| 17 | 15.529 | 1.70 | Ethanol, 1-(2-butoxyethoxy)- | Diethylene glycol n-butyl ether | C8H18O3 |
| 18 | 17.766 | 0.50 | Benzoic acid, 4-methyl- | Methyl benzoate | C8H8O2 |
| 19 | 18.531 | 2.07 | 2-Pentenoic acid, 4-hydroxy- | Levulinic acid | C5H8O3 |
| 20 | 18.757 | 3.20 | 2(5H)-Furanone, 3,5,5-trimethyl- | Allyl methacrylate | C7H10O2 |
| 21 | 19.217 | 5.98 | Furan, tetrahydro-2,2,4,4-tetramethyl- | Tetrahydrofuran | C8H16O |
| 22 | 20.472 | 2.34 | 4-Methyl-4-(tetrahydropyran-2-yl)oxypentane-2,3-dione | – | C11H18O4 |
| 23 | 21.182 | 1.38 | Decanoic acid, ethyl ester | Lauric acid | C12H24O2 |
| 24 | 22.443 | 7.33 | Benzaldehyde, 2-hydroxy-4-methyl- | Methyl benzoate | C8H8O2 |
| 25 | 23.827 | 0.77 | 1,3-Cyclohexanediol, 2,5-dimethyl-2-nitro-, diacetate (ester), (1.alpha.,2) | Glutaconylcarnitine | C12H19NO6 |
| 26 | 24.157 | 1.46 | Phenol, 2,4-bis(1,1-dimethylethyl)- | 2,4-Di-tert-butylphenol | C14H22O |
| 27 | 28.564 | 1.88 | Phenol, 2,6-dimethoxy-4-(2-propenyl)- | 2,4-Diethoxybenzaldehyde | C11H14O3 |
| 28 | 28.818 | 0.83 | Acetic acid, (3-allyloxy-1,1-dimethylbutyl) ester | Ethyl 2-acetylheptanoate | C11H20O3 |
| 29 | 29.363 | 12.21 | 4-((1E)-3-Hydroxy-1-propenyl)-2-methoxyphenol | Coniferyl | C10H12O3 |
| 30 | 30.046 | 1.62 | 9,10-Dimethyltricyclo[4.2.1.1(2,5)]decane-9,10-diol | Geranyl acetate | C12H20O2 |
| 31 | 32.017 | 0.90 | 1,2-Benzenedicarboxylic acid, bis(2-methylpropyl) ester | Dibutyl phthalate | C16H22O4 |
| 32 | 32.569 | 0.85 | 2,4-Dimethoxybenzyl alcohol | 1,2,4-Trimethoxybenzene | C9H12O3 |
| 33 | 33.735 | 10.31 | n-Hexadecanoic acid | Palmitic acid | C16H32O2 |
| 34 | 37.432 | 2.59 | Octadecanoic acid | Stearic acid | C18H36O2 |
| 35 | 38.178 | 2.91 | Andrographolide | Andrographis | C20H30O5 |
| 36 | 38.327 | 2.86 | 3.alpha.,17.beta.-dihydroxyestr-4-ene | Stearidonic acid | C18H28O2 |
| 37 | 40.555 | 1.12 | 9,19-Cyclolanost-23-ene-3,25-diol, 3-acetate, (3.beta.,23E)- | (20RS)-3β-Acetoxylupan-29-al | C32H52O3 |
| 38 | 43.182 | 1.70 | Hexadecanoic acid, 2-hydroxy-1-(hydroxymethyl)ethyl ester | Glyceryl palmitate | C19H38O4 |
| 39 | 44.351 | 1.32 | Butanoic acid, 2-methyl-, 2-methoxy-4-(2-propenyl)phenyl ester | Parthenolide | C15H20O3 |
| 40 | 45.848 | 1.18 | Phenol, 2-methoxy-4-(1-propenyl)-, acetate | Acetyleugenol | C12H14O3 |

Therefore, we evaluated the expression of the cyclin genes CCND1, CDK2, CDK4 and CDK6. The treatments showed inhibition of the tested cyclins, which are important cell cycle regulators that promote cell proliferation and growth cell (Besson et al., 2008). These results suggest a strong correlation between the decrease in the number of cells and the induction of cell cycle arrest.

CDKs coordinate cell cycle progression and their activity has been linked to a variety of diseases through the dysregulation of cell cycle control. The CDKI (CDK-interacting protein/kinase inhibitor protein) family of proteins is involved in cell cycle regulation, transcriptional regulation, apoptosis and cell migration (Amani et al., 2021). After determining that ET and F1 treatments were able to decrease cyclin levels, we investigated the CDKIs p53, p21, p16 and p27. These CDKIs did not show an increase in expression when treated with ET and F1, and this was not the way by which CDKs were downregulated. However, the p27 gene, whose main function is to bind and inhibit cyclinE/CDK2 complexes and also cyclinD/CDK4-6 complexes (Amani et al., 2021), was increased with treatment, suggesting the mechanism by which CCA occurred, consequently decreasing the proliferation of GRX cells.

An interesting finding described by Amani et al. (2021) demonstrated that p27, when expressed in lymphomas, causes a decrease or maintains the normal expression of p53 and p16. These data corroborate our findings in this study, where GRX cells treated with ET and F1 maintained unaltered p53 levels and decreased p16 compared to control.

A decrease in the expression pattern of cell cycle regulators is associated with overexpression of BCL-2 in quiescent cells or with abnormally increased proliferation. BCL-2-dependent upregulation of p27 inhibits the CyclinE/CDK2 complex, and thus decreases cell cycle progression (Du et al., 2021; Ghatei et al., 2017; Tsukamoto et al., 2006). BCL-2 affects the cell cycle at the transition between the G0/G1 and S phases or during the G2/M phase (Martins et al., 2015). Inhibition of the G1/S transition by BCL-2 overexpression occurs by modulating the level of proteins, such as p27, involved in the control of the G1/S transition. This effect may be reinforced by the inhibitory action that BCL-2 overexpression may have on multiple signaling pathways involved in the control of cell proliferation (Ghatei et al., 2017). Our results showed an increase in BCL-2 gene expression, corroborating these results.

The p27 protein binds and inhibits cyclin-CDK complexes in the nucleus, inducing cell cycle arrest. Notably, cytoplasmic p27 has been reported to promote macroautophagy/autophagy in response to nutrient shortages (Nowosad et al., 2021). Recent findings have found that, during prolonged amino acid starvation, p27 promotes autophagy via an mTOR-dependent pathway (Nowosad et al., 2021). Therefore, p27 represses MTORC1 activity, leading to nuclear translocation of the TFEB transcription factor and activation of lysosomal function, increasing the autophagic flow (Nowosad et al., 2021). Therefore, p27 represses MTORC1 activity, leading to nuclear translocation of the TFEB transcription factor and activation of lysosomal function, increasing the autophagic flow (Nowosad et al., 2021). Thus, the evaluation of the
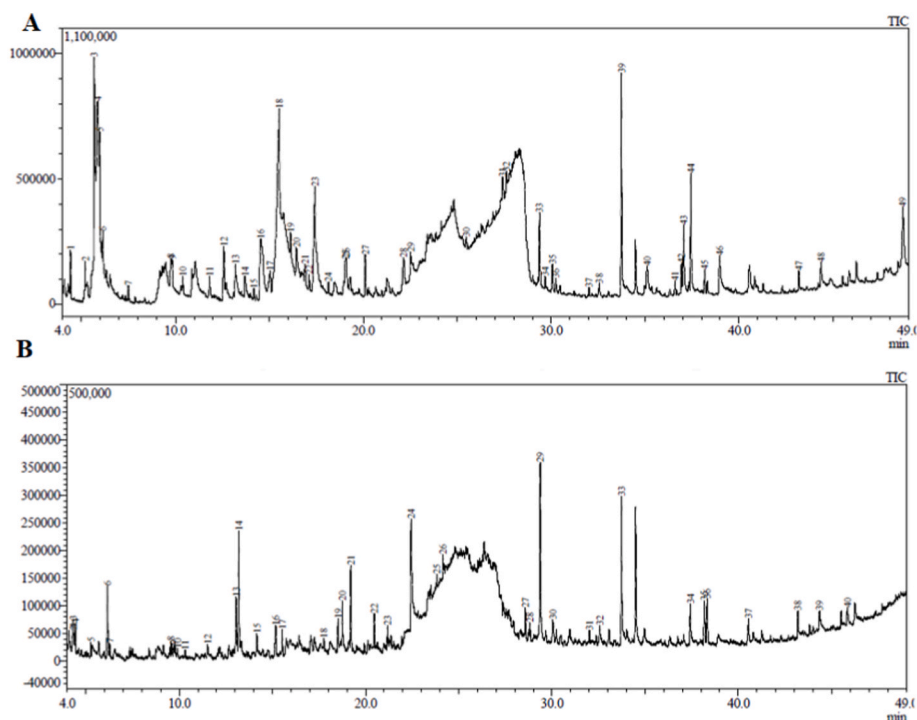
**Fig. 11.** GCMS analysis of ET (A) and F1 (B) compounds from *M. polymorphum*.

autophagic process by ET and F1, through the formation of AVOs, suggests an increase in lysosomal content in the cellular response induced by treatment with ET and F1 in GRX cells, suggesting a possible autophagic process.

The p27 protein is considered one of the main inhibitory molecules of the cell cycle and, therefore, controller of cell proliferation. Moreover, recent studies have shown that p27 induce inhibition of the mTOR signaling pathway in case of nutrient starvation and provoke a cell proliferation arrest in G1/S. This study also showed that, prolonged amino acid withdrawal, the cell-cycle inhibitor p27 exerts a direct negative feedback on the master cell growth regulator mTOR by participating in its inhibition, illustrating the crosstalk between the cell division and cell growth machineries (Nowosad et al., 2021). To corroborate the p27 gene expression increased by our treatment, we evaluated mTOR protein expression. Our results demonstrated that both ET and F1 caused a significant decrease in mTOR, showing that our treatment was able to increase P27 gene expression, which may have caused a decrease in mTOR, showing an important relationship between the decrease in key molecule in cell proliferation (mTOR) and its relationship with the increase in p27 protein. Our treatment appears to play an important role in mediating growth arrest by mTOR via the upregulation of p27.

HSCs, when in a quiescent state, accumulate retinol (vitamin A) in cytoplasm, and are known as lipocytes. These cells exert the function of maintaining the hepatic tissue and synthesizing proteins responsible for the formation and degradation of liver tissue ECM components (Borojevic et al., 1985; Iredale, 2008). Oil Red O staining allows for the visualization of lipid deposits in the GRX intracellular contents, and changes in cell morphology can be observed under phase-contrast microscopy. GRX cells treated with ET and F1 lost their elongated appearance and acquired a larger, polygonal shape, while control cells preserved their myofibroblast-like morphology and had few lipid droplets. These results show that our treatments had an antiproliferative effect and could deactivate HSCs, transforming the fibroblastic phenotype into quiescent cells.

PPARγ is a transcription factor related to quiescent phenotype induction in HSCs (Tsukamoto et al., 2006). To investigate the mechanism

involved in quiescent phenotype restoration, PPARγ mRNA expression was evaluated, showing that PPARγ gene expression was increased by treatment with ET and F1, suggesting a possible restoration of HSC quiescence. The non-alteration of PPARγ mRNA expression in NAC treatment seems to coincide with the literature, since its effect is mainly related to PPAR-α expression (Calzadilla et al., 2011).

To determine the possible effects of treatments on the HSCs phenotype, TGF-β, α-SMA and Col-1 profibrotic gene expression levels were investigated. The results show that the mRNA expression of these genes and de expression of α-SMA protein were suppressed by treatment with ET and F1. The cytokine TGF-β is a growth-related factor and plays a key role in HF development, mainly by activating quiescent HSCs, suppressing the characteristic of accumulating vitamin A in the cytoplasm and thus increasing cell contractility (Hernandez-Gea and Friedman, 2011). The ability to contract HSCs is related to increased α-SMA expression, since this actin isoform increases in myofibroblasts and has a fundamental role in the development of the fibrotic response. Another factor that is characterized by an increase in activated fibroblasts is the production of Col-1, which increases collagen deposition and thus tissue contracts more. These indicates a modulating effect of the treatments on the HSC phenotype, which may lead from an activated to a quiescent state.

ET and F1 extracts were phytochemically analyzed and showed different profiles, however, some compounds appear in both extracts. Among the major compounds in common between ET and F1, we can mention Coniferyl, which is an anti-inflammatory agent already used by the pharmaceutical industry, as well as in the treatment of liver cancer (He et al., 2021; Wang et al., 2020; Yao et al., 2018). ET presented Ethyl acetoacetate as one of its major compounds that is used in the production of a wide variety of anti-inflammatory compounds, which may be related to our findings (Amani et al., 2021; Farghaly et al., 1990; Fayed et al., 2021). Another compound that is part of the ET and corroborates our findings is Valeric acid, which affects several cancer-related pathways, such as liver cancer, through cell cycle arrest (Han et al., 2020; Park et al., 2016; Shi et al., 2021). F1 presented Adipic acid as one of its major compounds and it has been described in the literature for the treatment of inflammatory diseases and cancer (O'Neill et al., 2019;

Tabasi et al., 2013).

## 5. Conclusion

Natural products have played an important role in the creation of new alternatives to drugs with anti-inflammatory and antifibrotic activities. Our *in vitro* analysis showed that ET and F1 reduced GRX cell proliferation without causing cytotoxicity. Furthermore, it is suggested that the antiproliferative effect is related to the induction of cell cycle arrest, mediated by the upregulation of the p27 pathway by total extract and fraction 1. This upregulation causes inhibition of CDKIs, thus triggering cell cycle arrest. These phenomena can be highlighted in the treated cells and can be attributed, to a certain extent, to the therapeutic potential provided to the compounds present in the extracts. Our results also show that treatments can modulate the activated HSCs phenotype by activating PPARγ and decreasing profibrotic genes. Finally, our results suggest that extracts obtained from *M. polymorphum* has a potential therapeutic effect against liver fibrosis, but more studies still need to be carried out to confirm the potential effect of *M. polymorphum* extracts against liver fibrosis, as *in vivo* models, but we can already observe an interesting effect *in vitro* model.

## CRediT authorship contribution statement

**Matheus Scherer Bastos:** performed all experiments, analyzed the data and wrote the manuscript with review and contributions, Formal analysis, Writing – review & editing, All authors approved the final manuscript. **Rafaela Mallmann Saalfeld:** helped in phenotypic reversal and gene expression experiments, helped during the gene expression experiments as well as writing the manuscript, All authors approved the final manuscript. **Bruna Pasqualotto Costa:** helped in phenotypic reversal and gene expression experiments, All authors approved the final manuscript. **Maria Claudia Garcia:** helped in W. Blot's experiments, All authors approved the final manuscript. **Krist Helen Antunes:** performed the flow cytometry experiments, All authors approved the final manuscript. **Kétlin Fernanda Rodrigues:** helped during the gene expression experiments as well as writing the manuscript, All authors approved the final manuscript. **Denizar Melo:** helped in W. Blot's experiments, All authors approved the final manuscript. **Eliane Romanato Santarém:** conceived and planned this project, Project administration, analyzed the data and wrote the manuscript with review and contributions, Formal analysis, Writing – review & editing, All authors approved the final manuscript. **Jarbas Rodrigues de Oliveira .:** conceived and planned this project, Project administration, analyzed the data and wrote the manuscript with review and contributions, Formal analysis, Writing – review & editing, All authors approved the final manuscript.

## Declaration of competing interest

The authors declare that they have no competing interests.

## Data availability

Data will be made available on request.

## Acknowledgments

This study was funded by the Coordenação de Aperfeiçoamento de Pessoal de Nível Superior (CAPES/Brazil; Financial Code 001), through fellowship of first author and by National Council for Scientific and Technological Development (CNPq/Brazil) (Grant#311424/2018-0). License for Research on Brazil's Biodiversity, CNPq#010852/2014-0 and Sistema Nacional de Gestão do Patrimônio Genético e do Conhecimento Tradicional Associado – SISGEN# ABAD620.

## References

Amani, J., Gorjizadeh, Nassim, Younesi, S., Najafi, M., Ashrafi, A.M., Irian, S., Gorjizadeh, Negar, Azizian, K., 2021. Cyclin-dependent kinase inhibitors (CDKIs) and the DNA damage response: the link between signaling pathways and cancer. DNA Repair 102, 103103. https://doi.org/10.1016/j.dnarep.2021.103103.

Bassiony, H., Sabet, S., Salah El-Din, T.A., Mohamed, M.M., El-Ghor, A.A., 2014. Magnetite nanoparticles inhibit tumor growth and upregulate the expression of P53/P16 in ehrlich solid carcinoma bearing mice. PLoS One 9, e111960. https://doi.org/10.1371/journal.pone.0111960.

Besson, A., Dowdy, S.F., Roberts, J.M., 2008. CDK inhibitors: cell cycle regulators and beyond. Dev. Cell 14, 159–169. https://doi.org/10.1016/j.devcel.2008.01.013.

Borojevic, R., Monteiro, A.N., Vinhas, S.A., Domont, G.B., Mourão, P.A., Emonard, H., Grimaldi, G., Grimaud, J.A., 1985. Establishment of a continuous cell line from fibrotic schistosomal granulomas in mice livers. In Vitro Cell. Dev. Biol. 21, 382–390. https://doi.org/10.1007/BF02623469.

Calzadilla, P., Sapocnik, D., Cosentino, S., Diz, V., Dicelio, L., Calvo, J.C., Guerra, L.N., 2011. N-acetylcysteine reduces markers of differentiation in 3T3-L1 adipocytes. Int. J. Mol. Sci. 12, 6936–6951. https://doi.org/10.3390/ijms12106936.

David, N.de, Mauro, M.de O., Gonçalves, C.A., Pesarini, J.R., Strapasson, R.L.B., Kassuya, C.A.L., Stefanello, M.É.A., Cunha-Laura, A.L., Monreal, A.C.D., Oliveira, R.J., 2014. Gochnatia polymorpha ssp. floccosa: bioprospecting of an anti-inflammatory phytotherapy for use during pregnancy. J. Ethnopharmacol. 154, 370–379. https://doi.org/10.1016/j.jep.2014.04.005.

de Mesquita, F.C., Bitencourt, S., Caberlon, E., da Silva, G.V., Basso, B.S., Schmid, J., Ferreira, G.A., de Oliveira, F. dos S., de Oliveira, J.R., 2013. Fructose-1,6-bisphosphate induces phenotypic reversion of activated hepatic stellate cell. Eur. J. Pharmacol. 720, 320–325. https://doi.org/10.1016/j.ejphar.2013.09.067.

de Moraes Gonçalves, V., Da Silveira Moreira, A., de Oliveira, P.D., 2019. Genus Moquiniastrum (Asteraceae): overview of chemical and bioactivity studies. Curr. Bioact. Compd. 15, 377–398. https://doi.org/10.2174/1573407214666180524094146.

de Oliveira Mauro, M., Matuo, R., de David, N., Strapasson, R.L.B., Oliveira, R.J., Stefanello, M.É.A., Kassuya, C.A.L., de Cepa Matos, M.F., Faria, F.J.C., Costa, D.S., 2017. Actions of sesquiterpene lactones isolated from Moquiniastrum polymorphum subsp. floccosum in MCF7 cell line and their potentiating action on doxorubicin. BMC Pharmacol. Toxicol. 18, 53. https://doi.org/10.1186/s40360-017-0156-3.

de Souza Basso, B., Haute, G.V., Ortega-Ribera, M., Luft, C., Antunes, G.L., Bastos, M.S., Carlessi, L.P., Levorse, V.G., Cassel, E., Donadio, M.V.F., Santarém, E.R., Gracia-Sancho, J., Rodrigues de Oliveira, J., 2021. Methoxyeugenol deactivates hepatic stellate cells and attenuates liver fibrosis and inflammation through a PPAR-γ and NF-kB mechanism. J. Ethnopharmacol. 280, 114433 https://doi.org/10.1016/j.jep.2021.114433.

Dooley, S., ten Dijke, P., 2012. TGF-β in progression of liver disease. Cell Tissue Res. 347, 245–256. https://doi.org/10.1007/s00441-011-1246-y.

Du, X., Xiao, J., Fu, X., Xu, B., Han, H., Wang, Y., Pei, X., 2021. A proteomic analysis of Bcl-2 regulation of cell cycle arrest: insight into the mechanisms. J. Zhejiang Univ. B 22, 839–855.https://doi.org/10.1631/jzus.B2000802.

Edlich, F., 2018. BCL-2 proteins and apoptosis: Recent insights and unknowns. Biochem. Biophys. Res. Commun. 500, 26–34. https://doi.org/10.1016/j.bbrc.2017.06.190.

Farghaly, A.M., Chaaban, I., Khalil, M.A., Bekhit, A.A., 1990. Non-steroidal antiinflammatory agents synthesis of novel 2-pyrazolyl-4(3H)-Quinazolinones. Arch. Pharm. (Weinheim) 323, 833–836. https://doi.org/10.1002/ardp.19903231004.

Fayed, E.A., Bayoumi, A.H., Saleh, A.S., Ezz Al-Arab, E.M., Ammar, Y.A., 2021. In vivo and in vitro anti-inflammatory, antipyretic and ulcerogenic activities of pyridone and chromenopyridone derivatives, physicochemical and pharmacokinetic studies. Bioorg. Chem. 109, 104742 https://doi.org/10.1016/j.bioorg.2021.104742.

Friedman, S.L., 2008. Mechanisms of hepatic fibrogenesis. Gastroenterology 134, 1655–1669. https://doi.org/10.1053/j.gastro.2008.03.003.

Ghatei, N., Nabavi, A.S., Toosi, M.H.B., Azimian, H., Homayoun, M., Targhi, R.G., Haghir, H., 2017. Evaluation of bax, bcl-2, p21 and p53 genes expression variations on cerebellum of BALB/c mice before and after birth under mobile phone radiation exposure. Iran. J. Basic Med. Sci. 20, 1037–1043. https://doi.org/10.22038/IJBMS.2017.9273.

Guarneire, G.J., Lima, N.M., Carli, G.P., Andrade de, T.J.A.S., Castro de, S.B.R., Alves, C.C.S., Carli, A.P., 2021. Ethnobotanical assessment in protected area from Brazilian Atlantic Forest. Res. Soc. Dev. 10, e15310413714 https://doi.org/10.33448/rsd-v10i4.13714.

Guimarães, E.L.M., Franceschi, M.F.S., Andrade, C.M.B., Guaragna, R.M., Borojevic, R., Margis, R., Bernard, E.A., Guma, F.C.R., 2007. Hepatic stellate cell line modulates lipogenic transcription factors. Liver Int. 27, 1255–1264. https://doi.org/10.1111/j.1478-3231.2007.01578.x.

Han, R., Nusbaum, O., Chen, X., Zhu, Y., 2020. Valeric acid suppresses liver cancer development by acting as a novel HDAC inhibitor. Mol. Ther. - Oncolytics 19, 8–18. https://doi.org/10.1016/j.omto.2020.08.017.

He, Y., Li, Q., Zhou, W., Gu, Y., Jiang, Y., 2021. Coniferyl aldehyde alleviates LPS-induced WI-38 cell apoptosis and inflammation injury via JAK2–STAT1 pathway in acute pneumonia. Allergol. Immunopathol. 49, 72–77. https://doi.org/10.15586/aei.v49i5.464.

Hernandez-Gea, V., Friedman, S.L., 2011. Pathogenesis of liver fibrosis. Annu. Rev. Pathol. 6, 425–456. https://doi.org/10.1146/annurev-pathol-011110-130246.

Iredale, J., 2008. Defining therapeutic targets for liver fibrosis: exploiting the biology of inflammation and repair. Pharmacol. Res. 58, 129–136. https://doi.org/10.1016/j.phrs.2008.06.011.

Kolios, G., 2006. Role of Kupffer cells in the pathogenesis of liver disease. World J. Gastroenterol. 12, 7413. https://doi.org/10.3748/wjg.v12.i46.7413.

Kumar, P., Nagarajan, A., Uchil, P.D., 2018. Analysis of cell viability by the lactate dehydrogenase assay. Cold Spring Harb. Protoc. 2018, 095497 https://doi.org/10.1101/pdb.prot095497.

Limeiras, S.M.A., Oliveira, B.C., Pessatto, L.R., Pesarini, J.R., Kassuya, C.A.L., Monreal, A.C.D., Cantero, W.B., Antoniolli-Silva, R., Antoniolli-Silva, A.C.M.B., Stefanello, M.E.A., Oliveira, R.J., 2017. Effects of Moquiniastrum polymorphum ssp floccosum ethnolic extract on colorectal carcinogenesis induced by 1,2-dimethylhydrazine. Genet. Mol. Res. 16 https://doi.org/10.4238/gmr16019518.

Martins, G.G., Lívero dos, F.A.R., Stolf, A.M., Kopruszinski, C.M., Cardoso, C.C., Beltrame, O.C., Queiroz-Telles, J.E., Strapasson, R.L.B., Stefanello, M.É.A., Oude-Elferink, R., Acco, A., 2015. Sesquiterpene lactones of Moquiniastrum polymorphum subsp. floccosum have antineoplastic effects in Walker-256 tumor-bearing rats. Chem. Biol. Interact. 228, 46–56. https://doi.org/10.1016/j.cbi.2015.01.018.

Nowosad, A., Jeannot, P., Callot, C., Creff, J., Perchey, R.T., Joffre, C., Codogno, P., Manenti, S., Besson, A., 2021. Publisher Correction: p27 controls Ragulator and mTOR activity in amino acid-deprived cells to regulate the autophagy–lysosomal pathway and coordinate cell cycle and cell growth. Nat. Cell Biol. 23 https://doi.org/10.1038/s41556-021-00741-7, 1048–1048.

O'Neill, E., Chiara Goisis, R., Haverty, R., Harkin, A., 2019. L-alpha-aminoadipic acid restricts dopaminergic neurodegeneration and motor deficits in an inflammatory model of Parkinson's disease in male rats. J. Neurosci. Res. 97, 804–816. https://doi.org/10.1002/jnr.24420.

Oliveira, R.J., de David, N., Pesarini, J.R., Nogueira, T.D., Kassuya, C.A.L., Strapasson, R.L.B., Stefanello, M.E.A., Monreal, A.C.D., Matuo, R., Antoniolli-Silva, A.C.M.B., 2016. Moquiniastrum polymorphum subsp floccosum extract: screening for mutagenic and antimutagenic activity. Genet. Mol. Res. 15 https://doi.org/10.4238/gmr15048976.

Park, J.H., Noh, S.M., Woo, J.R., Kim, J.W., Lee, G.M., 2016. Valeric acid induces cell cycle arrest at G1 phase in CHO cell cultures and improves recombinant antibody productivity. Biotechnol. J. 11, 487–496. https://doi.org/10.1002/biot.201500327.

Park, Y.J., Kim, D.M., Jeong, M.H., Yu, J.S., So, H.M., Bang, I.J., Kim, H.R., Kwon, S.-H., Kim, K.H., Chung, K.H., 2019. (–)-Catechin-7-O-β-d-Apiofuranoside inhibits hepatic stellate cell activation by suppressing the STAT3 signaling pathway. Cells 9, 30. https://doi.org/10.3390/cells9010030.

Pereira-Filho, G., Ferreira, C., Schwengber, A., Marroni, C., Zettler, C., Marroni, N., 2008. Role of N-acetylcysteine on fibrosis and oxidative stress in cirrhotic rats. Arq. Gastroenterol. 45, 156–162. https://doi.org/10.1590/S0004-28032008000200013.

Piornedo, R. dos R., de Souza, P., Stefanello, M.É.A., Strapasson, R.L.B., Zampronio, A.R., Kassuya, C.A.L., 2011. Anti-inflammatory activity of extracts and 11,13-dihydroza-luzanin C from Gochnatia polymorpha ssp. floccosa trunk bark in mice. J. Ethnopharmacol. 133, 1077–1084. https://doi.org/10.1016/j.jep.2010.11.040.

Roehlen, N., Crouchet, E., Baumert, T.F., 2020. Liver fibrosis: mechanistic concepts and therapeutic perspectives. Cells 9, 875. https://doi.org/10.3390/cells9040875.

Schuppan, D., Ashfaq-Khan, M., Yang, A.T., Kim, Y.O., 2018. Liver fibrosis: direct antifibrotic agents and targeted therapies. Matrix Biol. 68 (69), 435–451. https://doi.org/10.1016/j.matbio.2018.04.006.

Shi, F., Li, Y., Han, R., Fu, A., Wang, R., Nusbaum, O., Qin, Q., Chen, X., Hou, L., Zhu, Y., 2021. Valerian and valeric acid inhibit growth of breast cancer cells possibly by mediating epigenetic modifications. Sci. Rep. 11, 2519. https://doi.org/10.1038/s41598-021-81620-x.

Stepanenko, A.A., Sosnovtseva, A.O., Valikhov, M.P., Chernysheva, A.A., Cherepanov, S.A., Yusubalieva, G.M., Ruzsics, Z., Lipatova, A.V., Chekhonin, V.P., 2022. Superior infectivity of the fiber chimeric oncolytic adenoviruses Ad5/35 and Ad5/3 over Ad5-delta-24-RGD in primary glioma cultures. Mol. Ther. - Oncolytics 24, 230–248. https://doi.org/10.1016/j.omto.2021.12.013.

Strober, W., 2001. Trypan blue exclusion test of cell viability. In: Current Protocols in Immunology. John Wiley & Sons, Inc., Hoboken, NJ, USA https://doi.org/10.1002/0471142735.ima03bs21.

Sui, X., Han, X., Chen, P., Wu, Q., Feng, J., Duan, T., Chen, X., Pan, T., Yan, L., Jin, T., Xiang, Y., Gao, Q., Wen, C., Ma, W., Liu, W., Zhang, R., Chen, B., Zhang, M., Yang, Z., Kong, N., Xie, T., Ding, X., 2021. Baicalin induces apoptosis and suppresses the cell cycle progression of lung cancer cells through downregulating akt/mTOR signaling pathway. Front. Mol. Biosci. 7 https://doi.org/10.3389/fmolb.2020.602282.

Tabasi, M., Amanlou, M., Siadat, S., Nourmohammadi, Z., Omoomi, F., Sadat Ebrahimi, S., Aghasadeghi, M., Rahimi, P., Pourhosseini, S., Mehravi, B., Ardestani, M., 2013. Novel molecular anti- colorectalcancer conjugate:chlorambucil-adipic acid dihydrizide-glutamine. Anti Cancer Agents Med. Chem. 13, 1449–1459. https://doi.org/10.2174/18715206113139990132.

Teixeira, M.P., Cruz, L., Franco, J.L., Vieira, R.B., Stefenon, V.M., 2016. Ethnobotany and antioxidant evaluation of commercialized medicinal plants from the Brazilian Pampa. Acta Bot. Bras. 30, 47–59. https://doi.org/10.1590/0102-33062015abb0150.

Teratake, Y., Kuga, C., Hasegawa, Y., Sato, Y., Kitahashi, M., Fujimura, L., Watanabe-Takano, H., Sakamoto, A., Arima, M., Tokuhisa, T., Hatano, M., 2016. Transcriptional repression of p27 is essential for murine embryonic development. Sci. Rep. 6, 26244 https://doi.org/10.1038/srep26244.

Tsukamoto, H., She, H., Hazra, S., Cheng, J., Miyahara, T., 2006. Anti-adipogenic regulation underlies hepatic stellate cell transdifferentiation. J. Gastroenterol. Hepatol. 21, S102–S105. https://doi.org/10.1111/j.1440-1746.2006.04573.x.

Wang, Y., Gao, Y., Li, X., Sun, X., Wang, Z., Wang, H., Nie, R., Yu, W., Zhou, Y., 2020. Coniferyl aldehyde inhibits the inflammatory effects of leptomeningeal cells by suppressing the JAK2 signaling. BioMed Res. Int. 2020, 1–12. https://doi.org/10.1155/2020/4616308.

Wynn, T.A., Ramalingam, T.R., 2012. Mechanisms of fibrosis: therapeutic translation for fibrotic disease. Nat. Med. 18, 1028–1040. https://doi.org/10.1038/nm.2807.

Yao, G.-D., Wang, J., Song, X.-Y., Zhou, L., Lou, L.-L., Zhao, W.-Y., Lin, B., Huang, X.-X., Song, S.-J., 2018. Stereoisomeric guaiacylglycerol-β-coniferyl aldehyde ether induces distinctive apoptosis by downregulation of MEK/ERK pathway in hepatocellular carcinoma cells. Bioorg. Chem. 81, 382–388. https://doi.org/10.1016/j.bioorg.2018.08.033.

Youssef, J., Döll-Boscardin, P.M., Farago, P.V., Duarte, M.R., Budel, J.M., 2013. Gochnatia polymorpha: macro- and microscopic identification of leaf and stem for pharmacognostic quality control. Rev. Bras. Farmacogn. 23, 585–591. https://doi.org/10.1590/S0102-695X2013005000054.

Zhang, Y., Kwok-Shing Ng, P., Kucherlapati, M., Chen, F., Liu, Y., Tsang, Y.H., de Velasco, G., Jeong, K.J., Akbani, R., Hadjipanayis, A., Pantazi, A., Bristow, C.A., Lee, E., Mahadeshwar, H.S., Tang, J., Zhang, J., Yang, L., Seth, S., Lee, S., Ren, X., Song, X., Sun, H., Seidman, J., Luquette, L.J., Xi, R., Chin, L., Protopopov, A., Westbrook, T.F., Shelley, C.S., Choueiri, T.K., Ittmann, M., Van Waes, C., Weinstein, J.N., Liang, H., Henske, E.P., Godwin, A.K., Park, P.J., Kucherlapati, R., Scott, K.L., Mills, G.B., Kwiatkowski, D.J., Creighton, C.J., 2017. A pan-cancer proteogenomic atlas of PI3K/AKT/mTOR pathway alterations. Cancer Cell 31, 820–832. https://doi.org/10.1016/j.ccell.2017.04.013 e3.